JEAS

Journal of Engineering and Applied Sciences 3 (2007) 15 – 20

JOURNAL OF ENGINEERING AND

An interpretation of total intensity aeromagnetic maps of part of southeastern Sokoto basin

A.Z. Labbo, F.X.O. Ugodulunwa*

*Geological Survey of Nigeria Agency, Kaduna *Department of Geology and Mining, University of Jos, Jos*

Abstract

The total magnetic field intensity maps of part of south-eastern Sokoto basin (1: 100,000 sheets 29, 30, 51 and 52) were digitized and processed. A composite total magnetic field intensity map of the four sheets was produced. Regional-residual separation, second vertical derivative calculation and two-dimensional spectral analysis were carried out. The residual field map and second vertical derivative (SVD) map showed discontinuities some of which coincide with the geological boundaries between marine sediments of Maastrichtian (Sokoto Group) and Palaeocene (Rima Group) and sediments of Quaternary (Illo/Gundummi). The two-dimensional spectral analysis indicated a two-depth source model. The deeper sources occurred at the depth of 1.25km - 1.80km while the shallower sources occurred at the depth of 0.31km – 0.56km. The deeper sources probably represent depths to the Pre-Cambrian basement and the shallower sources probably represent depths to the magnetized bodies within the sediments. The surface plot of the depths to the basement shows some narrow depressions in the basement, which constitute sub-basins. The faults and fractures are potential channels for mineralization fluids. The sub-basins can play host to sedimentary mineral deposits.

1. Introduction

Sokoto Basin is located at the south-eastern section of the intracontinental sedimentary Iullemmeden basin, which extends from Mali and western boundary of Niger Republic through northern Benin Republic and north-western Nigeria into the eastern Niger Republic (Kogbe, 1979). The study area is in the southeastern part of the Sokoto Basin (Fig. 1). It lies between longitudes 5.00^{o}E and 6.00^{o}E and latitudes 12.00^{o}N and 13.00^{o}N. The main features of the study area are the "Dange scarps" and the low regional dip of about 2^{o} with west-north-west trend, (Carter, 1964; Kogbe, 1979). The present interpretation of the total magnetic field intensity map of this part of Sokoto Basin will aid the evaluation of the mineral potential of the area, assist in the program of geological mapping of the area and help elucidate its subsurface structure.

Geology and water resources

The study area is underlain by Pre-Cambrian Basement Complex rocks (gneisses, quartzite, and phyllite) and Mesozoic and Tertiary sediments (Fig. 2). Rocks of the Basement Complex outcrop in the southeastern extremity of the study area. The sediments include the Illo and Gundumi formations, Rima and Sokoto Groups, and the Gwandu formation. These sediments had been affected by series of marine transgressions, and were deposited during three main phases of deposition, (Kogbe, 1979). The first phase was during the continental period when Illo and Gundumi Formations were deposited unconformably on the Pre-Cambrian Basement Complex. The Illo and Gundumi Formations are made up of grits and clays, which form part of the Continental Intercalair of West Africa. The second phase began with the Maastrichtian transgression which continued into the Palaeocene (Adeleye, 1979) and resulted in the deposition of the Rima Group (Maastrichtian) and the Sokoto Group (Palaeocene). The third and the final phase began in early Eocene with the regression of the sea. Continental conditions prevailed while the Gwandu Formation of Eocene to Miocene age was laid down. These Continental conditions continued to prevail until the present day. The sediments dip gently and thicken gradually towards the northwest, with a maximum thickness of over 1,000 meters near Nigeria's frontier with Niger Republic

(Zabek and Emecheta, 1982). Highly metamorphosed sediments occur at the boundary between the Basement rocks and the Cretaceous sediments. These metasediments consist of calc-silicate rocks, quartzites and high grade schist (Etu-Effeotor, 1998). Boulders of rocks of the Older Granite suite are widespread in this area.

A number of economic mineral deposits occur in the study area. For example gypsum and phosphate deposits occur in the shales of Dange Formation (of Sokoto Group) and Dukamaje Formation (of Rima Group). These deposits extend to Malbaza in Niger Republic (Agbata, 1989). The mudstones and siltstones in Wurno Formation (of Rima Group) and Gamba Formation (of Sokoto Group) also contain small lumps of gypsum. The occurrence of gypsum in Sokoto Basin was first reported in the sediments of the Rima valley (Falconer, 1911).

The study area has a relatively flat topography and is drained by River Sokoto and its tributaries. River Sokoto flows southwards and empties into the River Niger. The main sources of water for agriculture are springs and streams, while industries rely on boreholes.

2. Materials and methods

The four aeromagnetic maps used for this work (1: 100,000 sheets 29, 30, 51 and 52) cover the south-eastern part of the Sokoto Basin. Each map was digitized and the data were combined to generate a single map of 10201 grid points at an equal spacing of 1.1km interval. The composite total intensity aeromagnetic map of the area was contoured at 10γ contour interval (Fig.3). It showed a prominent northeast-southwest trend of linear anomalies and some high gradient anomalies. These structures may help to understand the geological setting of the area.

2.1. Method of analysis

In the analytical interpretation, frequency domain filtering processes were applied to the total intensity magnetic field data. These include matched regional/residual filter, second vertical derivative calculation and spectral analysis. These resulted in transforming the data into residual field maps, second vertical derivative map and plot of the basement surface topography. The contouring of maps and plot of Basement surface was achieved with Surfer Package of Golden Software Incorporation and the colour-shaded maps were generated with the Oasis Montaj Software of Geosoft Technology. Colour-shaded maps were also produced. The intervals between contour lines are represented by a range of colours of the natural colour spectrum: red (high) through orange, yellow, green and blue (low) (Reeves, 2005). Colour shaded maps reveal at once the difference between 'highs' and 'lows'.

2.2. Regional-residual separation

The observed magnetic field at every point is a vector sum of various components, such as the regional field component and the local field component. In addition to induced magnetism, rocks may also have remanent magnetic component (Clark, 1997). Remanent magnetism is the effect of the primary magnetic field at the time of rock formation. The total magnetic response is proportional to both the induced magnetism as well as remanent magnetism (Luendy, 1997). The regional field was assumed to be a first order polynomial plane (Fig.4). It was derived by least-square fitting of a plane: $T(x,y) = (a_o + a_1x + a_2y)$ where x and y are unit spacing along the two axes of the blocks and the coefficient a_o, a_1 and a_2 are 7831.8560, -24.1014 and –7.8135 respectively. From this relation the regional gradients along any line were calculated. This was achieved with the aid of *fortran* program *pf2.for*, which is based on least square (best-fit polynomial).The computed regional magnetic field was subtracted from the digitized data to obtain the residual magnetic field which reflects local geological events (Figs. 5 and 6).

2.3. Second vertical derivatives

Derivatives provide a useful way of highlighting small features with steep gradients. Vertical derivatives of the magnetic field can be computed by multiplying the amplitude spectra of the field by a factor of the form:

$$1/\eta[(n^2 + m^2)^{1/2}]^{\eta}$$

where η is the order of the vertical derivative (or vertical gradient). The vertical derivative is physically equivalent to measuring the magnetic field simultaneously at two points vertically above each other, subtracting the data and dividing the result by the vertical spatial separation of the measurement points. The second vertical derivative is the vertical gradient of the first vertical derivative and so on. The frequency response formula of these operations shows that the process enhances high frequencies relative to low frequencies and this property is the basis for the application of the derivatives processes to eliminate long-wavelength regional effects and resolve the effects of the adjacent anomalies (Milligan and Gunn, 1997).

Apart from enhancing the shallower anomalies the second vertical derivatives are also used to delineate geological boundaries between rocks with contrast in physical properties such as magnetic susceptibility. The contoured second vertical derivative outlines the bodies causing the magnetic anomalies. The zero contours which usually mark these outlines are more visible than on the original map, where they may be obscured by large changes in the magnetic field. The center of a uniform gradient band taken from the profiles will often be close to zero derivative contour. This center line actually lies close to inflection points, where the second vertical derivative is zero in the direction of the profiles, provided that there are no gradient

changes perpendicular to the profiles. It therefore corresponds to the flanks of long bodies. The second vertical derivative calculation was achieved with the aid of *fortran* program *SVD.for*, using fast-fourier transform (FFT). The second vertical derivative map enhanced all shallow effects observed in the residual map (Figs. 7 and 8).

2.4. Spectral analysis

Fourier analysis is used for the estimation of the depth to sources of potential field in the earth's crust. In this work the aeromagnetic data is represented by two-dimensional Fourier series consisting of various frequencies, which characterize the anomalies.

The residual map was divided into four blocks each 32 ×32 in dimension. As described by Hahn et al. (1976), the following criteria were kept in mind while choosing the dimensions of the blocks:

1. Each block should contain more than one maximum or minimum;
2. The square's sides should not cut through the essential parts of the anomalies. Each map had been digitized at an equal spacing of 1.1km, yielding 2601 data values.

The residual field values were represented by a double Fourier series expansion;

$$\Delta T(x,y) = \sum_{n=0} \sum_{m=-M} P^n_m \cos[(2\pi/L)(nx + my)] + \varphi^n_m \sin[(2\pi/L)(nx + my)]$$

Where L = length of the square side, $\mathbf{P}^n_m$ and $\boldsymbol{\varphi}^n_m$ are the Fourier amplitude, N, M = number of grid points along x and y directions. The sum in the above relation represents a single partial wave for which the amplitude is:

$$(P^n_m)^2 + (\varphi^n_m)^2 = (\psi^n_m)^2$$

Where ψ^n_m is the amplitude of the partial wave whose frequency is given by

$$f^n_m = \sqrt{(n^2 + m^2)}$$

The average amplitude spectrum of all waves falling within a given frequency range is then computed by summing the Fourier amplitudes and dividing the sum by the number of frequencies. The average amplitudes of all blocks were plotted on semi-log paper against the frequency. The spectrum showed two straight-line segments in two frequency ranges. While the line segment in the higher frequency range is from the shallower sources the lower harmonics appeared from the deeper sources.

The slope of the segment is related to the depth by the relation; $Z = SL/2\pi$. (Hahn et.al, 1976). The average depth estimate in each block was made by the above formula. Table 1 shows the result obtained from the analysis. The two-dimensional spectral analysis of the magnetic data was achieved with the aid of *fortran* program *spt.for*.

3. Results and discussion

Magnetic anomalies observed in the aeromagnetic maps are due to magnetized bodies at different depths. The area is totally overlain by sedimentary rocks of different ages. Sedimentary rocks generally have low susceptibilities than the underlying basement rocks. Therefore the long wavelength magnetic anomalies are usually associated with the basement while the short wavelength anomalies are mainly due to the presence of magnetized bodies at shallower depths.

1) The magnetic intensity of the magnetic sources is generally high in the southwestern, central and northern parts of the study area and low in northwestern part (Figs.3 and 6).
2) The residual magnetic field (the field due to short wavelength anomalies and/or shallow features) contain anomalies and magnetic discontinuities with dominant NE-SW and E-W trends (Figs.5and6). The field due to long wavelength anomalies or deeper magnetic features trends generally in the NW-SE direction (Fig.3). This corresponds to one of the three linear belts described by Umego et. al (1992).
3) The most prominent anomaly with low magnetic intensity in the northern part of the study area has a value of about -160γ. It traverses the entire breadth of the area immediately north of Lat $12^o50'$N and continues northeastwards outside the study area (Fig.6). A major NW-SE discontinuity occurs between the northwestern and central sections of the magnetic zone, west of longitude 5.50^0E.
4) The discontinuities on the residual magnetic field map may be interpreted as contacts between different lithologic units or fractures/faults within the Basement. When compared with the geological map of the area (Fig.2). It will be noticed that the Sokoto Group underlies the area with low magnetic intensity in the northwest. The Rima Group, Illo Formation and Gundumi Formation underlie the areas with varied magnetic intensity in the northern, central and southwestern parts of the study area.The NW-SE discontinuity in the northern part of the study area probably corresponds with one of the geological contacts between the Sokoto Group and the Rima Group, near Dange and Shuni towns. The magnetic low around Bodinga occurs over Gwandu Formation. The two NE-SW trending discontinuities in the southwestern part of the study area probably correspond with the contact between the Quarternary Illo/Gundumi Formation and the Basement Complex in the southeast and the Palaeocene sediments of the Rima Group to the northwest.

5) The result of the two-dimensional spectral analysis (Table1) indicated a two-depth source model. The deeper sources occur at the depth of 1.25km - 1.80km while the shallower sources occur at the depth of 0.35km – 0.45km. The deeper sources probably represent the depth to the Pre-Cambrian Basement and the shallower sources probably represent the depth to the magnetized bodies within the sediments. This result is quite reasonable when compared with the result obtained by Umego et. al (1995). The surface plot of the depths to the basement shows some narrow depressions in the basement, which can be attributed to the presence of faults or fractures in the Basement (Fig. 9).The depressions constitute sub-basins. The deeper depressions occur below the Rima Group. They are linked, and seem to be bounded by a strong NE-SW trending discontinuity. This discontinuity may be a fracture zone within the Basement Complex.

Table 1.
Depths to magnetic sources in southeastern part of Sokoto Basin

D = 1.80	D = 1.73	D = 1.35	D = 1.40
S = 0.35	S = 0.38	S = 0.44	S = 0.43
D = 1.59	D = 1.54	D = 1.54	D = 1.49
S = 0.36	S = 0.56	S = 0.42	S = 0.31
D = 1.52	D = 1.28	D = 1.42	D = 1.49
S = 0.43	S = 0.44	S = 0.40	S = 0.46
D = 1.45	D = 1.25	D = 1.51	-
S = 0.41	S = 0.42	S = 0.43	-

[D = Deeper sources, S = Shallow sources in km.]

4. Conclusion

The result of the spectral analysis revealed the existence of shallow (0.3km – 0.56km) and deep (1.25 – 1.80) depressions in the Basement Complex. These occur in the central and southwestern parts of the study area which is underlain mainly by sediments of the Rima Group. The deepest depressions occur in the southwest. They are bounded by a NW-SE trending discontinuity that may correspond to a fracture zone within the Basement Complex. Such a fracture zone will provide a channel for mineralizing fluids to get to the overlying sediments. The depressions constitute sub-basins that can host mineral deposits. The residual magnetic anomaly map and the second vertical derivative maps show dominant NE-SW discontinuities. Some E-W trends have also been observed. These discontinuities correspond to fractures, faults or lithological boundaries.

Acknowledgements

The authors would like to thank the Geological Survey of Nigeria Agency, Kaduna for releasing the aeromagnetic maps for this study. We also thank Prof. A. N. Umego for providing some materials from his work in the study area.We are also grateful to Prof. I. B. Osazuwa and Dr Kola Lawal of Physics Department A. B. U Zaria, and Mr S. M Anka (Late) of Physics Department, Usmanu Dan-Fodio University, Sokoto for their assistance during the digitizing and processing of the aeromagnetic maps used for this work. We also thank Geosoft Europe, Wallingford – Oxford U. K. for providing temporary licence of Oasis Montaj software, which was used in the data processing.

References

Adeleye, D. R., 1979. A review of Maastritchian paleogeography of the southern Iullemmeden and Nupe Basins. Nigeria Journal of Mining and Geology, pp.10-14.

Agbata, P. C., 1989. Gypsum in the Dukamaje and Dange Formations of the Rima River, Sokoto Basin. M.Sc.Thesis, A. B. U. Zaria, pp.42-48.

Carter, J. D., 1964. A Note on the sedimentary rocks of the Northern part of Sokoto Province. No. 55, pp.20-21.

Clark, D. A., 1997. Magnetic petrology aid to geological interpretation of Magnetic Data. AGSO Journal of Australian Geology and Geophysics, pp.83-103.

Falconer, J. D., 1911. The Geology and Geography of Northern Nigeria. Macmillan, London, 295p.

Geological Survey of Nigeria, 1984. Geological map of Nigeria

Hahn A., Kind E. G., and Mishra, D. C., 1976. Depth estimation of magnetic sources by means of Fourier amplitude spectra. Geophysical Prospecting 24, pp.287-308.

Jones, B., 1948. Sedimentary rocks of Sokoto Province. Geological Survey of Nigeria Bulletin, 18, 79p.

Kogbe, C. A., 1979. Geology of the south-eastern sector (Sokoto) of the Iullemmeden Basin. Department of Geology bulletin, A. B. U. Zaria, 420p.

Luendy, A. P. J., 1997. Processing of airborne magnetic data. AGSO Journal of Australian Geology and Geophysics, 17,2, pp.31-38.

Milligan, P. R., Gunn, P. J., 1997. Enhancement and presentation of airborne geophysical data. AGSO Journal of Australian Geology and Geophysics, 17,2, Pp.175 – 185.

Reeves, C., 2005. Gridded data, Maps, Images and Enhancements. 22p Geowitch 1411 Lk Naarden, The Netherlands

Umego, M. N., Ojo S. B., Ajakaiye, D. E., 1995. Magnetic depth to basement analysis in the Sokoto Basin, Northwestern Nigeria. Nigeria Journal of Mining and Geosciences (NMGS), 31,2, pp.161-168.

Umego, M. N., Ojo S. B., Dyrelius D., Ajakaiye D. E., 1992. Composite magnetic anomaly map of the Sokoto Basin, Northwestern Nigeria. Nigeria Journal of Mining and Geology, 28,2, pp. 309-315.

Zabek, J., Cassat, G. Emencheta, J. C., 1982. ELF Aquitaine Nigeria Services Report on the exploration for hydrocarbons in the Sokoto Basin. Exploration Department, Lagos. 25p.

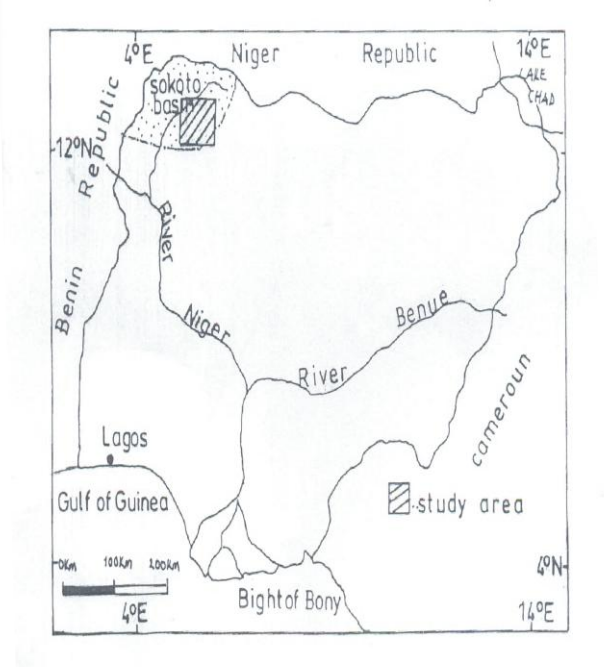

Fig.1. Simplified map of Nigeria showing the location of the study area.

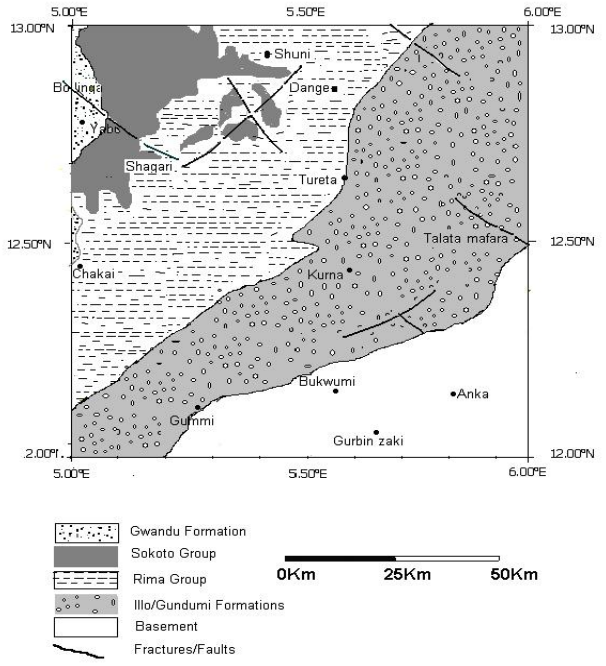

Fig. 2. Geological map of southeastern part of Sokoto basin (After Geological Survey of Nigeria, 1984).

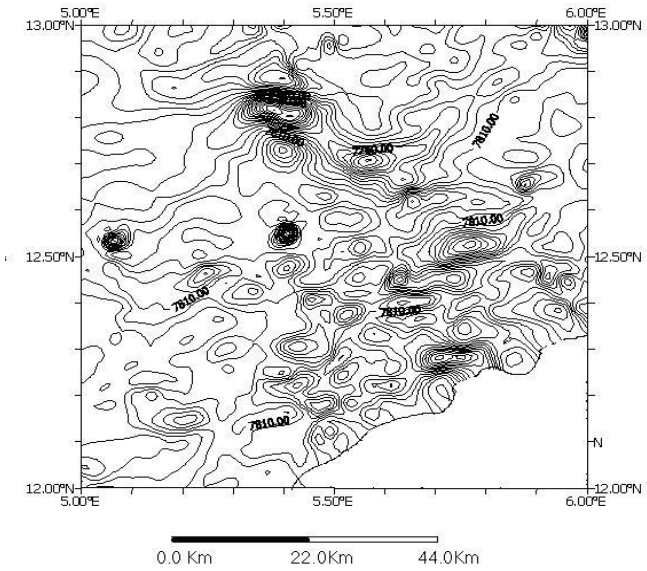

Fig. 3. Total Intensity map of southeastern part of Sokoto basin contour intervals = 10γ.

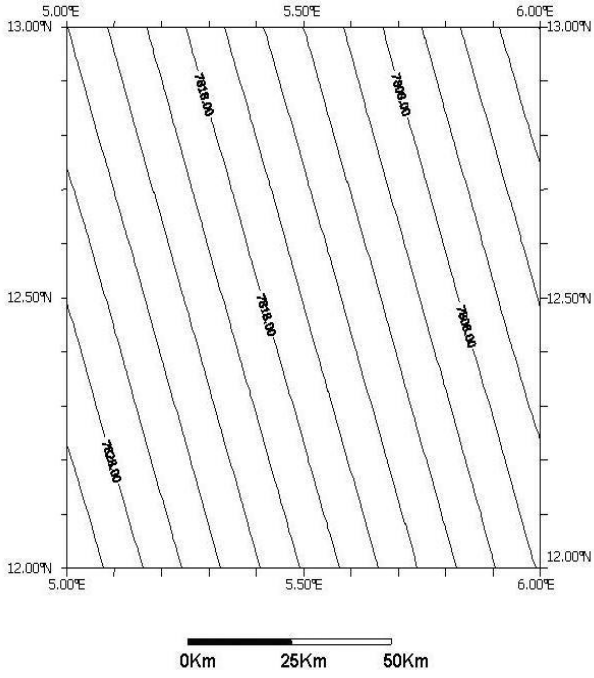

Fig. 4. Map of assumed regional magnetic field of southeastern part of Sokoto basin (First order polynomial plane surface) contour interval = 10 gamma.

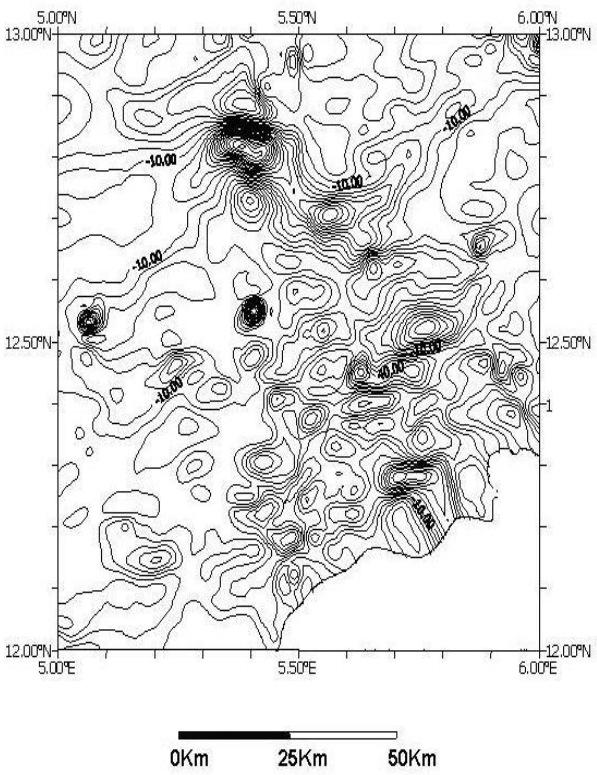

Fig. 5. Residual magnetic intensity map of southeastern part of Sokoto basin contour intervals = 10 gamma.

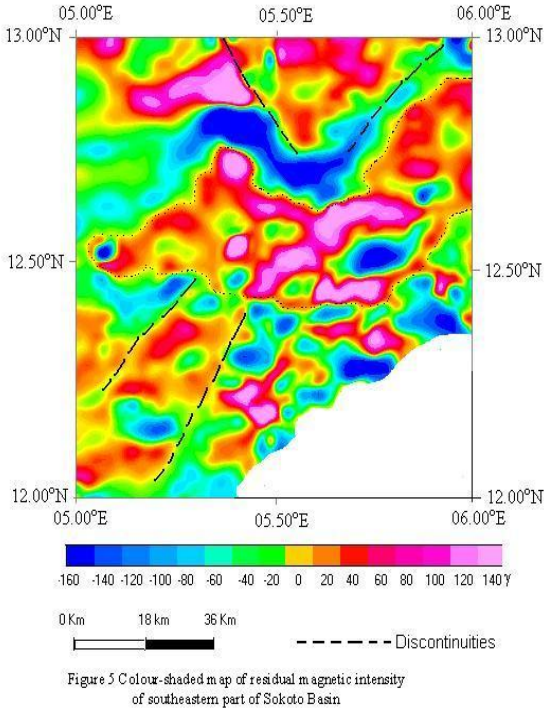

Fig. 6. Colour-shaded map of residual magnetic intensity of southeastern part of Sokoto basin.

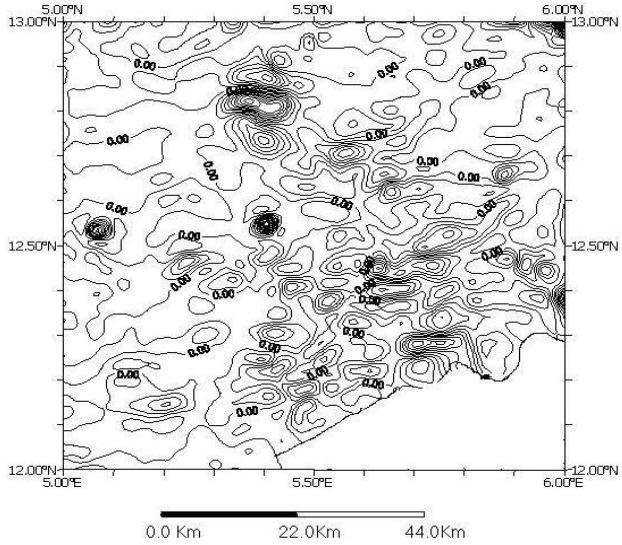

Fig. 7. Second vertical derivative map of southeastern part of Sokoto basin. contour intervals = 1γ.

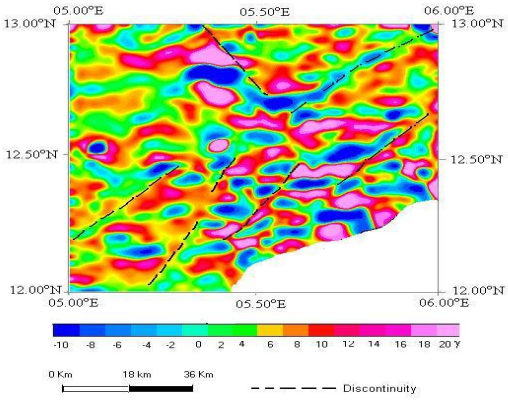

Fig. 8. Colour shaded map of second vertical derivative map of Southeastern part of Sokoto basin

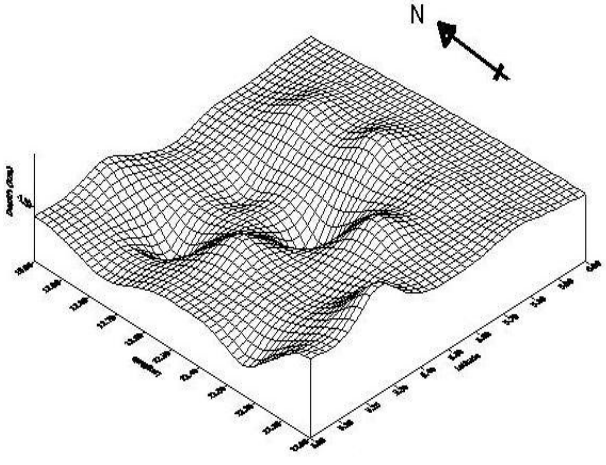

Fig. 9. Plot of the basement surface of southeastern part of Sokoto basin.